CORE
Metadata, citation and similar papers at core.ac.uk
Provided by City Research Online

City Research Online

City, University of London Institutional Repository

Citation: Davenport, J. J., Hickey, M., Phillips, J. P. & Kyriacou, P. A. (2017). Dual pO_2/pCO_2 fibre optic sensing film. The Analyst, 142(10), pp. 1711-1719. doi: 10.1039/C7AN00173H

This is the accepted version of the paper.

This version of the publication may differ from the final published version.

Permanent repository link: http://openaccess.city.ac.uk/17560/

Link to published version: http://dx.doi.org/10.1039/C7AN00173H

Copyright and reuse: City Research Online aims to make research outputs of City, University of London available to a wider audience. Copyright and Moral Rights remain with the author(s) and/or copyright holders. URLs from City Research Online may be freely distributed and linked to.

City Research Online: http://openaccess.city.ac.uk/ publications@city.ac.uk

Dual pO_2/pCO_2 fibre optic sensing film

John J. Davenport, * Michelle Hickey, Justin P. Phillips and Panayiotis A. Kyriacou

A fibre optic multi-sensor has been developed for biomedical sensing applications using a tip coating solution sensitive to both oxygen and carbon dioxide. An oxygen sensitive phosphorescence quenching complex based on platinum octaethylporphyrin (PtOEP) was combined with a carbon dioxide sensitive phosphorescence compound based on 8-hydroxypyrene-1,3,6-trisulfonic acid trisodium salt (HPTS). When excited by blue light (470 nm), the resultant coating had two fluorescent peaks at 515 nm (green) and 645 nm (red) which responded to partial pressure of CO_2 and O_2 respectively. The sensor was tested *in vitro* and shown to be able to measure CO_2 and O_2 simultaneously and in real time, with calibration constants of 0.0384 kPa^{-1} and 0.309 kPa^{-1} respectively. The O_2 sensitive peak received some overlap from the 515 nm peak (0.38% of peak intensity) as well as some cross-sensitivity (maximum, 5.1 kPa pCO_2 gave a measurement equivalent to 0.43 kPa of O_2, a ratio of 0.08 : 1). However, these effects can be subtracted from measurements and no significant cross-sensitivity or overlap was seen in CO_2 measurements from O_2. This novel compound presents great potential for use in medical sensors and we expect it to be important to a wide range of future applications.

1. Introduction

Background

In this study a fibre-optic sensor has been developed using a novel chemical coating sensitive to both pO_2 and pCO_2, allowing simultaneous measurements with a single system. Previous studies have demonstrated fibre optic sensors for measurement of pO_2 [1–3] and pCO_2 [4–6] in isolation, while some sensors and coating layers have been developed into commercially available products.[7–10] Fibre optic sensors have advantages over other types of sensors in that they are chemically inert, able to reach difficult locations, and provide electrical isolation from optoelectronic components, reducing the risk of electrocution. These advantages are particularly useful for biomedical applications.

Despite clear potential benefits, pO_2 and pCO_2 sensors have not been combined onto a single optical fibre. In this study we have developed a novel sensor which uses a chemical coating containing both pO_2 and pCO_2 sensitive materials. Combining measurements of both gases in a single fibre allows more comprehensive assessment of respiratory gas exchange in biological tissue. Simultaneous measurement of pO_2 and pCO_2 will provide information regarding the uptake of oxygen and carbon dioxide production within biological systems, which will provide insight into respiratory and metabolic processes. The combination of both measurements suggest multiple laboratory applications including measurements of cellular respiration *in vitro*, as well as analysis of gas partial pressures in blood and body fluid samples. It will also find multiple applications as an *in vivo* biomedical sensor, particularly monitoring pO_2 and pCO_2 in the interstitial fluid. The sensor described in this paper was developed with this application in mind, specifically to provide continuous monitoring of pO_2 and pCO_2 in the gastrointestinal epithelium for estimation of the perfusion status of the gut. Such measurements provide early warning of impending gut ischaemia which can lead to deterioration of intensive care patients' conditions including development of sepsis, septic shock and multiple organ dysfunction.[11] Other applications could include transcutaneous gas concentration measurements,[12,13] as well as measurement of inspired and expired respiratory gas concentrations,[14] either incorporated into an anaesthetic breathing circuit or directly from the mouth, nose or trachea.

Chen *et al.*[15] developed a fibre optic pO_2 sensor based on PtOEP and a cylindrical core optical fibre. The sensor was optimised for rapid measurements showing a minimum response time of less than 50 ms. Yang *et al.*[16] developed a pO_2 sensor on microstructured polymer optical fibre segments tris (4,7-diphenyl-1,10-phenathroline) ruthenium(II) dichloride ($[Ru(dpp)_3]Cl_2$). The sensor gave a ratio of fluorescent intensities between pure N_2 and pure O_2 of 10.8. Bukowski *et al.*[17] developed a sensor material based on tris(4,7-diphenyl-1,10-phenathroline) ruthenium(II) ($[Ru(dpp)_3]^{2+}$). Coated onto a microscope slide it gave a ratio of fluorescent intensities between pure N_2 and pure O_2 of 35.

Research Centre for Biomedical Engineering, University of London, Northampton Square, London, EC1V 0HB, UK. E-mail: john.davenport.1@city.ac.uk

For pCO_2, Chu *et al.*[4] Developed a fibre optic sensor based on 1-hydroxy-3,6,8-pyrenetrisulfonic acid trisodium salt (HPTS), finding a limit of detection of 0.03%. Contreras-Gutierrez *et al.*[18] developed a pCO_2 fibre optic sensor using a polymer matrix in which a fluorescent dye is combined directly with the polymer molecule, showing a limit of detection of 0.4% CO_2. Segawa *et al.*[19] developed a similar fibre optic sensor using thymol blue with a minimum detected CO_2 concentration of 0.2%.

This study builds on the work of Chen *et al.* and Chu *et al.* develop a novel chemical mix which, when coated onto the tip of an optical fibre, produces a sensor capable of responding to both pO_2 and pCO_2 simultaneously. The coating avoids adverse interactions between the various components involved and maintains performance with minimal cross-sensitivity. This development presents many new opportunities for biomedical and other sensing applications.

2. Theory

pO_2 measurement

Measurement of the partial pressure of oxygen in this system is based on phosphorescence quenching, using the molecule PtOEP. Phosphorescence occurs when a molecule, referred to as a fluorophore, absorbs a photon of one wavelength, entering an excited state, and then re-emits a photon of a different wavelength at a later point. The absorption and the re-emission wavelengths are both characteristic of the specific molecule.

Phosphorescence quenching occurs when excitation energy is transferred from the fluorophore to another chemical, referred to as a quencher. The fluorophores are therefore unable to emit phosphorescent photons and the intensity of phosphorescent light decreased.

There are many mechanisms for this energy transfer including collision quenching, charge transfer or the formation of static complexes. Here, we focus on collision quenching, one of the most common types and the mechanism responsible for oxygen quenching of PtOEP.[15] In collision quenching the fluorophore and the quencher interact and energy is transferred to the quencher. This prevents the fluorophore decaying photo-chemically and emitting its photons.

By observing the decrease in phosphorescence intensity, the concentration of the quencher can be ascertained. In the simplest case of a single collision-quenching path in a homogenous environment, the phosphorescence intensity change caused by quenching is given by:[15]

$$I = \frac{I_0}{1 + K_{sv}[O_2]} \quad (1)$$

where I is the phosphorescence intensity in the presence of oxygen, I_0 is the intensity in its absence, K_{sv} is the Stern–Volmer constant and $[O_2]$ is the oxygen concentration. K_{sv} is specific to the combination of fluorophore and quencher and is equal to the product of τ_0, the lifetime of the excited fluorophore and k, the bi-molecular rate.

The values of I_0 and K_{sv} depend on the intensity and coupling efficiency of the excitation light source, the quantity and concentration of the fluorophore, temperature of the environment and the specific efficiency of collisions between PtOEP and oxygen. The values of I_0 and K_{sv} can be found for a given device to allow oxygen concentration to be calculated.

pCO_2 measurement

Based on phosphorescence indication of pH changes associated with dissolved CO_2. The fluorophore can absorb light of 480 nm and re-emit light of 520 nm.[18] In the presence of CO_2 and a transfer agent, a series of equilibrium reactions take place, decreasing the concentration of the fluorophore. The concentration of CO_2 can be found from the intensity of the emitted light.

The interaction between the fluorophore, TONOH and dissolved CO_2 is shown in Scheme 1.[20] Here, DH is the protonated form of the fluorophore and D^- is the deprotonated form.

The first line shows the interaction between the TONOH and the fluorophore before the sensor is exposed to the sample. The second line shows the interaction between CO_2 and TONOH. The third line shows the interaction between the reaction products of the first two lines. Therefore, when TONOH is abundant, the ratio of DH to D^- is dependent on the quantity of CO_2.[20]

When excited, DH fluoresces at 520 nm. The greater the concentration of exited fluorescent molecules, the greater the phosphorescence intensity. Provided sufficient TONOH was included, by shifting the concentration of DH, CO_2 decreases the intensity of fluorescent light resulting from excitation. The resultant intensity follows a relationship similar to the Stern–Volmer relationship described above.[4]

$$I = \frac{I_0}{1 + \alpha[CO_2]} \quad (2)$$

where $[CO_2]$ is the carbon dioxide concentration, α is a calibration constant incorporating equilibrium constants for the interactions shown in Scheme 1, and other symbols have the same meanings as above. The values of I_0 and α can be found for a given device to allow carbon dioxide concentration to be calculated.

$$DH + TONOH \cdot xH_2O \rightleftharpoons D^-TON^+ \cdot xH_2O + H_2O$$

$$CO_2 + TONO \cdot xH_2O \rightleftharpoons HCO_3^-TON^+ \cdot xH_2O$$

$$D^-TON^+ \cdot xH_2O + HCO_3^-TON^+ \cdot xH_2O \rightleftharpoons CO_3^{2-}(TON^+)_2 \cdot 2xH_2O + DH$$

Scheme 1 Chemical interaction between the fluorophore, TONOH and dissolved CO_2.

3. Materials and methods

Sensor fabrication and setup

The combined pCO_2/pO_2 sensor was made by dip coating a polymer layer containing materials sensitive to CO_2 and to O_2 onto the distal tip of an optical fibre. The tip was then placed in contact with a sample. The interaction between the sensing layer and O_2 or CO_2 in the sample allowed the partial pressures of the two gases to be measured.

Fig. 1 shows a diagram of the distal tip of the sensor. The sensing layer contains PtOEP, a fluorescent molecules sensitive to pCO_2 and HTPS, a fluorescent molecule that can be transferred to a non-fluorescing form by CO_2 when in the presence of the transfer agent TONOH. Both molecules were excited by blue (460 nm) light, provided by an LED coupled to the proximal end of the fibre. Exited PtOEP fluoresced red (645 nm) depending on the concentration of O_2 and HTPS fluoresced green (515 nm) depending on the concentration of CO_2. The fluorescent wavelength of 515 nm observed in this study is slightly shorter than usual HPTS peak wavelength of 520 nm. This difference is discussed in more detail later. By analysing the spectrum of the light returning from the sensor, the partial pressure of CO_2 and O_2 could be ascertained.

Preparation and application of the sensing film

The following chemicals were used to create the coating solution: platinum octaethylporphyrin (PtOEP, $Pt(NC_9H_{11})_4$, CAS: 31248-39-2) as the oxygen sensitive fluorophore, poly(ethyl methacrylate) (PEMA, $[CH_2C(CH_3)(CO_2C_2H_5)]_n$, CAS: 9003-42-3) as a fixer, dichloromethane (CH_2Cl_2 CAS: 75-09-2) as a solvent, 8-hydroxypyrene-1,3,6-trisulfonic acid trisodium salt (HPTS, $C_{16}H_7Na_3O_{10}S_3$, CAS: 6358-69-6) as the CO_2 sensitive fluorophore, 1-ethyl-3-methylimidazolium tetrafluoroborate ($EMIMBF_4$, CAS: 143314-16-3) to stabilise the HPTS and tetraoctylammonium hydroxide solution (TONOH, $C_{32}H_{69}NO$, CAS: 17756-58-0, supplied in 20% solution with methanol) as a phase transfer agent. All three were obtained from Sigma-Aldrich Corporation, St Louis, USA.

PtOEP (1.0 mg) and PEMA (102 mg) powder was mixed with CH_2Cl_2 liquid (1.6 ml) in a glass vial, which was left to stand until the powders had completely dissolved. HPTS (5.0 mg) powder was then added. The ionic liquid $EMIMBF_4$ (0.1 ml) was added to stabilise the HPTS and increase its lifetime, as described by Oter *et al.*[21] Finally, TONOH solution (0.4 ml) was added and the vial was left to stand to allow the HPTS to dissolve.

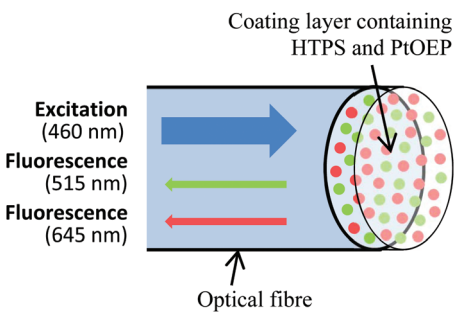

Fig. 1 The distal tip of the sensor, including a coating layer containing HTPS and PtOEP molecules. Both are excited by blue (460 nm) light. HTPS fluoresces green (515 nm), decreasing with increasing pCO_2. PtOEP fluoresces red (645 nm) decreasing with increasing pO_2.

The chemical coating was applied using a precision dip coater (precision dip coater, model – QPI-168, Qualtech Products Industry, Denver, USA). It was set to lower the tip of the optical fibre (BFL48-600 fibre, 600 μm fibre core, 0.48 NA, Ocean Optics, Dunedin, USA) into a vial of coating solution and then withdraw it at a rate of 1 nm s^{-1}, allowing 30 minutes for the solvent to evaporate. After which, a coating of coat of silicone rubber was applied (CS2 condensation cure, Easy Composites, Stoke-on-Trent, UK, using MED-160 primer, Nusil Silicon Technology, Carpinteria, USA) and left to set for 24 hours.

Chemical mix development

The chemical mix used to create the sensing was described above. Before this mix was finalised a number of other preliminary alternatives were tried in order to ensure the composition worked and performed as desired. Table 1 shows the makeup of the mixes that were tested before finalising the mix used for this study.

Early iterations of the mix, the CO_2 signal at 515 nm decayed rapidly, within a few hours of use, limiting the function of the sensor. Varying the concentration of $EMIMBF_4$ helped to increase the lifetime of the sensor, but had the potential of forcing the PEMA out of solution where it formed solid crystals in mixing vial.

The order at which components were added was also important. It was found that PtOEP would not dissolve in a solution containing methanol, such as that added with the TONOH, but it would remain in solution if first dissolved in CH_2Cl_2 in advance of adding methanol (at least in the concentrations used here).

Finally, once a working mix had been obtained, several more compositions were tested in order to optimise the performance and maximise the strength of CO_2 and O_2 signals. By increasing the intensity of return signals from the sensor, its accuracy and limit of detection was expected to increase.

Numerous studies have been done on theoretically or experimentally determining the thickness of a smooth film dip-coated onto a surface,[22,23] however they typically assume a vertical surface withdrawn from the coating. Fig. 2 shows a microscope image of the chemical mix coated onto the tip of an optical fibre. It can clearly be seen that surface is not flat or smooth with numerous creases.

It is believed that these are caused by a small droplet forming at the tip of the fibre, which then shrinks as the solvents evaporate. Thakur *et al.*[24] tested a PEMA based coating similar to the one described in this study, deposited by spray pyrolysis. Similar creases were observed when zing oxide nanoparticles were introduced, also attributed to shrinkage during evaporation of the solvent. Thakur *et al.* observed a refractive

Table 1 Details of preliminary chemical mix compositions tested before finalising to the mix used in this study. Components were added in the quantities and orders listed, and solids were given time to dissolve between each step they were added to a solvent

Batch	Details	Observations
1a	0.7 mg PtOEP, 1.6 ml CH_2CL_2, 0.1 ml $EMIMBF_4$, 102 mg PEMA, 0.4 ml TONOH in methanol, 40 mg HPTS	Strong CO_2 peak that decayed rapidly (few hours).
1b	0.7 mg PtOEP, 100 mg PEMA, 9.8 mg HPTS, 1.6 ml CH_2CL_2.	Solids did not dissolve fully.
1c	0.5 mg PtOEP, 102 mg PEMA, 1.6 ml CH_2CL_2, 0.1 ml $EMIMBF_4$, 5 mg HPTS.	—
1d	0.1 mg PtOEP, 101 mg PEMA, 1.6 ml CH_2CL_2, 0.1 ml $EMIMBF_4$, 1.5 mg HPTS.	HPTS did not dissolve.
1e	0.1 mg PtOEP, 100 mg PEMA, 1.6 ml CH_2CL_2, 1.5 mg HPTS, 0.4 ml TONOH in methanol, 0.1 ml $EMIMBF_4$.	HPTS appeared to dissolve better after TOHON was added. CO_2 peak decays. A further 0.1 ml $EMIMBF_4$, peak still decays.
1f	0.9 mg PtOEP, 101 mg PEMA, 1.6 ml CH_2CL_2, 0.4 ml TONOH in methanol, 105 mg Polym H7, a matrix forming polymer bonded to fluorescent molecules as well as TONOH.	CO_2 peak decayed.
1g	0.9 mg PtOEP, 100 mg PEMA, 0.4 ml CH_2CL_2, 1.2 ml methanol, 0.4 ml TONOH in methanol, 1.5 mg HPTS.	PEMA crystals formed on adding methanol, but dissolved on shaking. No O_2 peak, CO_2 peak decayed
1gII	0.6 mg PtOEP, 100 mg PEMA, 0.4 ml CH_2CL_2, 1.2 methanol, 0.1 ml $EMIMBF_4$, 2 mg HPTS.	As before, PEMA crystals formed but dissolved when shaken.
2h	—	
2a	1 mg PtOEP, 0.2 ml $EMIMBF_4$, 1.5 ml CH_2CL_2, 0.2 ml TONOH in methanol.	—
2b	Vial 1: 102 mg PEMA, 1 mg PtOEP, 0.4 ml CH_2CL_2. Vial 2: 0.2 ml $EMIMBF_4$, 1.5 ml methanol, 0.2 ml TONOH in methanol. Vial 1 then added to vial 2, then 1.7 mg HTPS	—
2c	Vial 1: 100 mg PEMA, 1 mg PtOEP, 0.4 ml CH_2CL_2. Vial 2: 1.5 ml methanol, 0.2 ml TONOH in methanol.	—
2d	100 mg PEMA, 0.5 mg PtOEP, 0.7 mg HPTS, 0.4 ml CH_2CL_2, 1.2 methanol, 0.4 ml TONOH in methanol, 0.1 ml $EMIMBF_4$.	HPTS did not dissolve. Some of the PEMA solidified or did not dissolve initially.
2e	101 mg PEMA, 0.5 mg PtOEP, 0.4 ml CH_2CL_2, 0.1 ml $EMIMBF_4$, 1.5 ml methanol, 0.2 ml TONOH in methanol, 0.1 mg HPTS.	Gave low but stable CO_2 peak, no O_2 signal.
2f	103 mg PEMA, 1.4 mg PtOEP, 0.4 ml CH_2CL_2, 1.5 ml methanol, 0.2 ml $EMIMBF_4$, 0.2 ml TONOH in methanol, 0.1 mg HPTS.	Low CO_2 signal, small O_2 peak.
2g	100 mg PEMA, 2 mg PtOEP, 0.5 ml CH_2CL_2, 1.5 ml methanol, 0.2 ml $EMIMBF_4$, 0.2 ml TONOH in methanol, 0.1 mg HPTS.	No signal at all.
2h	100 mg PEMA, 0.1 mg PtOEP, 0.5 ml CH_2CL_2, 1.5 ml methanol, 0.2 ml $EMIMBF_4$, 0.2 ml TONOH in methanol, 0.2 mg HPTS.	Medium signal for both CO_2 and O_2.
3	1000 mg PEMA, 1.5 mg PtOEP, 5 ml CH_2CL_2, 15 ml methanol, 2 ml $EMIMBF_4$, 2 ml TONOH in methanol, 8 mg HPTS.	Similar behaviour to 5p.
4	9.9 mg PtOEP, 1003 mg PEMA, 16 ml CH_2CL_2, 15 mg HPTS, 1 ml $EMIMBF_4$, 4 ml TONOH in methanol.	—
4a	3 mg PtOEP, 101 mg PEMA, 1.6 ml CH_2CL_2, 15 mg HPTS, 0.1 ml $EMIMBF_4$, 0.4 ml TONOH in methanol.	—
4b	1 mg PtOEP, 102 mg PEMA, 1.6 ml CH_2CL_2, 5 mg HPTS, 0.1 ml $EMIMBF_4$, 0.4 ml TONOH in methanol.	Gives strong and stable peaks for both CO_2 and O_2.
4c	1 mg PtOEP, 100 mg PEMA, 0.4 ml CH_2CL_2, 5.1 mg HPTS, 0.1 ml $EMIMBF_4$, 0.4 ml TONOH in methanol, 0.2 methanol	No O_2 peak.
4d	1 mg PtOEP, 100 mg PEMA, 1.6 ml CH_2CL_2, 5 mg HPTS, 0.2 ml $EMIMBF_4$, 0.4 ml TONOH in methanol	—

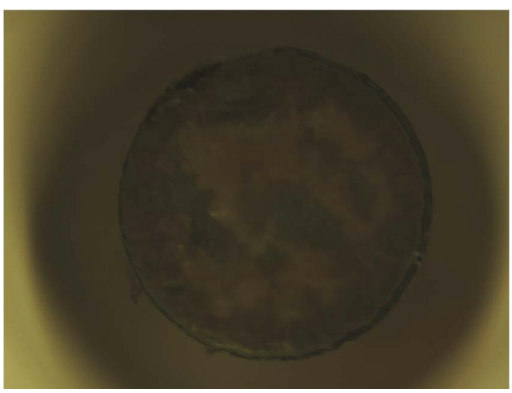

Fig. 2 Microscope image (20× magnification) of the chemical mix coated onto the tip of a 600 μm optical fibre.

index of PEMA coatings to vary between 1.55 and 1.59, depending on the deposition time of the coating.

These may influence the performance of the sensors as light reaching the surface will tend to scatter rather than reflect evenly. However, this sensor method does not rely on reflection or coating thickness for its function, rather that excitation light reaches the HTPS and PtOEP, and phosphorescent light transmits, reflects or scatters back. Variations in the surface properties of the coating are expected to affect only the calibration of the sensor, not its basic function.

System setup

Sensors were mechanically spliced to an optical fibre splitter (bifurcated borosilicate fibre, 600 μm diameter multi-mode

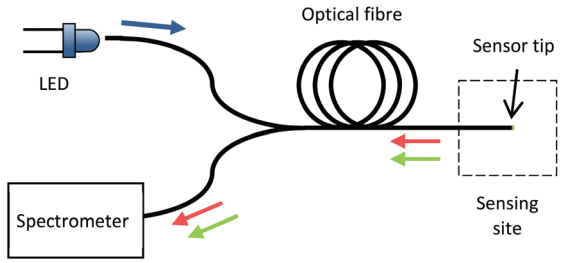

Fig. 3 Diagram of the optical layout of the sensor. The fibre splitter allows light from the LED to reach the sensing layer and excite the fluorophores, and fluorescent light to pass back to the spectrometer.

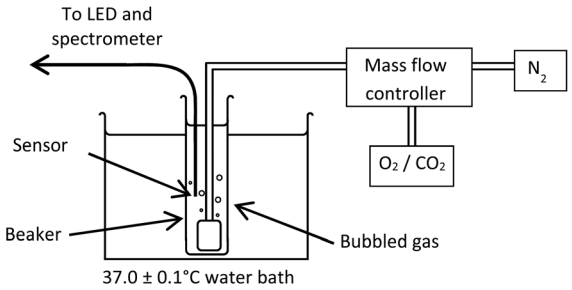

Fig. 4 Diagram of the setup used for in-vitro testing of the sensors. Oxygen concentration was controlled by bubbling gas through the water in the conical flask.

core, BIFBORO-600-2 supplied by Ocean Optics) connected to an LED (460 nm, Wurth Elektronik, 151033BS03000, RS Components, UK) and a spectrometer (Ocean Optics Flame miniature spectrometer), using a 50 ms integration time and averaging over 100 measurements throughout this study. Fig. 3 shows a diagram of the optical layout of the system.

Blue light (460 nm) was introduced to the optical fibre using an LED, which then passed through the fibre splitter to the sensing layer. The LED had a luminous intensity of 3.8 cd and couples an estimated 1.4 mW of light into the optical fibre. The fluorescent components of HPTS fluoresced green (515 nm) with decreasing intensity in the presence of CO_2. PtOEP fluoresced red (645 nm) with decreasing intensity in the presence O_2. The fibre splitter delivered this light to the spectrometer. By measuring the intensity of green and red light from the sensor the partial pressure of CO_2 and O_2 to be ascertained.

In vitro testing

The sensors were tested *in vitro*. The sensor was inserted into a narrow beaker containing distilled water in order to measure the effects of changing pO_2 and pCO_2. The partial pressures were controlled by bubbling gas through an aerator and allowing the dissolved gases to equilibrium. The gas input was provided by combining flow from an N_2 cylinder, a CO_2 cylinder and an O_2 cylinder (supplied by BOC, USA). The beaker was placed within a water bath (Fisher Scientific 12777819 – Thermostatic circulator bath) kept at 37.0 ± 0.1 °C. This mimicked human body temperature as well as ensuring that temperature changes did not affect the sensing layer. A diagram of the *in vitro* setup is shown in Fig. 4.

Flow rates were measured and controlled using mass flow controllers (FMA-A2406-SS-(N_2) mass flow controller, supplied by Omega Engineering, US). Concentrations of CO_2 and O_2 were controlled by varying the ratios of flow with N_2. Preliminary testing found that with this setup, dissolved gas concentrations reached equilibrium within three minutes. Five minutes was therefore given to allow a margin of error. A baseline measurement of 100% N_2 was recorded between each O_2 or CO_2 measurement.

First, a sensor was tested using under varying oxygen conditions whilst keeping the carbon dioxide concentration at zero, followed by testing a sensor under varying carbon dioxide conditions while keeping the oxygen concentration at zero. This allowed the sensitivity to oxygen and carbon dioxide to be tested separately, and cross-sensitivity of each of the fluorescent peaks to be identified.

Details of the flow rates used for these tests are given in Tables 2 and 3. Partial pressures were calculated from gas percentages assuming a standard atmospheric pressure of 101.3 kPa.

4. Results

Fig. 5 shows the spectrum of light returning from the sensor at varying levels of pCO_2, normalised to the excitation light from

Table 2 Variation pO_2 in determined by flow rates of O_2 and N_2. Each gas mix was permitted to flow for five minutes to allow the concentration in the water to reach equilibrium and a baseline measurement of 100% N_2 was recorded between each O_2 measurement

O_2 (ml min^{-1})	N_2 (ml min^{-1})	O_2 (%)	pO_2 (kPa)
0	500	0 ± 3	0 ± 3
100	400	20 ± 3	20 ± 3
200	300	40 ± 3	41 ± 3
300	200	60 ± 3	61 ± 3
400	100	80 ± 3	81 ± 3
450	50	90 ± 3	91 ± 3
500	0	100 ± 3	101 ± 3

Table 3 Variation pCO_2 in determined by flow rates of CO_2 and N_2. Each gas mix was permitted to flow for five minutes to allow the concentration in the water to reach equilibrium and a baseline measurement of 100% N_2 was recorded between each CO_2 measurement

CO_2 (ml min^{-1})	N_2 (ml min^{-1})	CO_2 (%)	pCO_2 (kPa)
0	500	0 ± 3	0 ± 3
15	485	3 ± 3	3.0 ± 3
25	475	5 ± 3	5.1 ± 3
50	450	10 ± 3	10 ± 3
100	400	20 ± 3	20 ± 3
200	300	40 ± 3	41 ± 3
300	200	60 ± 3	61 ± 3

the LED is centred at 470 nm reflected from the sensor tip. The peak from the LED is truncated in this graph as it is not the focus of this study. The phosphorescence signal from the CO_2 sensitive material HTPS is centred at 515 nm, where it can be seen to decrease in intensity with increasing concentration, as expected.

The peak at 645 nm is the phosphorescence signal from the O_2 sensitive material PtOEP. It shows some CO_2 cross-sensitivity to O_2 measurements, which will be discussed in more detail later. It is also noticeable that there is a dip in intensity from the CO_2 sensitive peak centred at around 539 mm which is not usually seen for HTPS.[18] Likewise the HTPS is usually observed at 520 nm as the peak is broader, without the dip at 539 nm.[18] This dip is believed to be caused by absorbance from the PtOEP included in the coating, and it was found to be absent when PtOEP was not included. However, provided measurements were taken from the shifted HTPS peak maximum at 539 nm, it was not found to be an issue.

The sensor spectrum for varying concentrations of oxygen is shown in Fig. 6. It can be seen that the 515 nm peak does not decrease as seen in Fig. 5, showing minimal O_2 cross-sensitivity to CO_2 measurements. The 645 nm is shown in more detail in Fig. 7 where it can be seen to drop off rapidly with increasing O_2 as expected. It can also be seen that there is a slight overlap between the 645 nm peak and the tail end of the 539 nm peak, which may lead to further cross-sensitivity.

Fig. 8 shows the intensity ration plot for the 515 nm peak for varying levels of pCO_2, along with a theoretical plot based on eqn (2). The results correspond well to theoretical predictions, with all values being within errors. Errors were found by combining the standard deviation of all baseline peak intensities with the standard deviation of phosphorescence intensity change measurements over a 3.1 nm range at the top of each peak. The calibration constant, α, was found empirically by a least squares fit to have a value of 0.0384 kPa^{-1}.

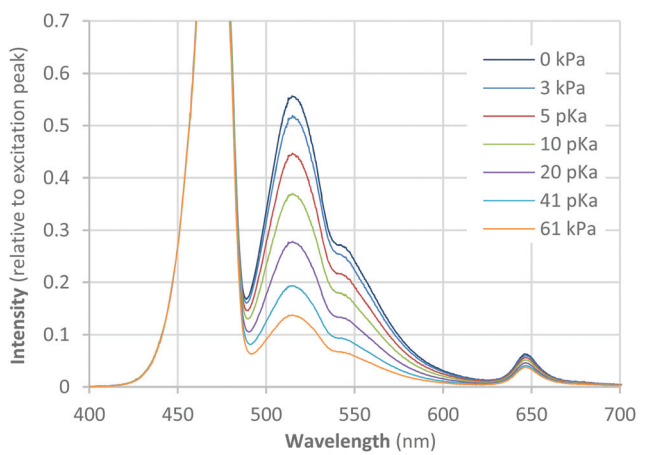

Fig. 5 Spectrum of light returning from the sensor at varying pCO_2. The truncated peak at 470 nm is the excitation peak from the LED reflecting off the sensor tip, the peak at 515 nm is the phosphorescence peak sensitive to CO_2 and the peak at 645 nm is the phosphorescence peak sensitive to O_2.

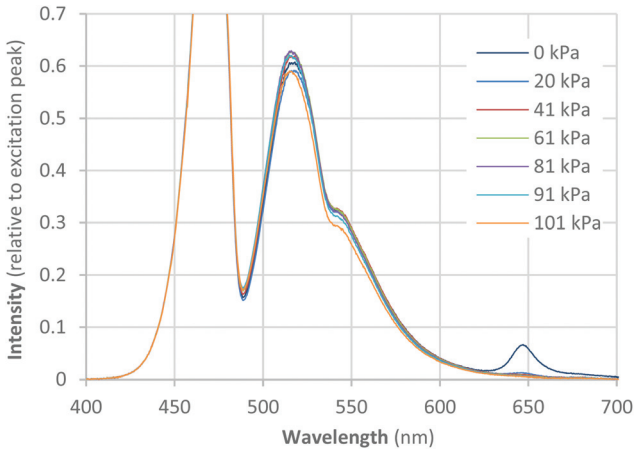

Fig. 6 Spectrum of light returning from the sensor at varying pO_2. The truncated peak at 470 nm is the excitation peak from the LED reflecting off the sensor tip, the peak at 515 nm is the phosphorescence peak sensitive to CO_2 and the peak at 645 nm is the phosphorescence peak sensitive to O_2.

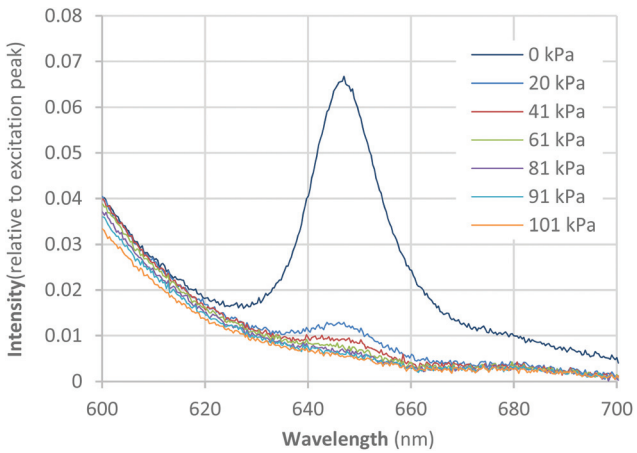

Fig. 7 Expansion of the O_2 sensitive phosphorescence peak at 645 nm at varying pO_2. The tip of the CO_2 sensitive peak can also be seen on the left side.

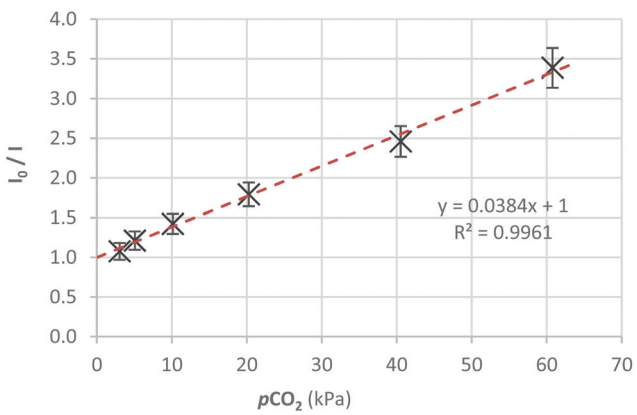

Fig. 8 Plot of the CO_2 sensitive phosphorescence peak at 515 nm against varying pCO_2. α = 0.0384 kPa^{-1}.

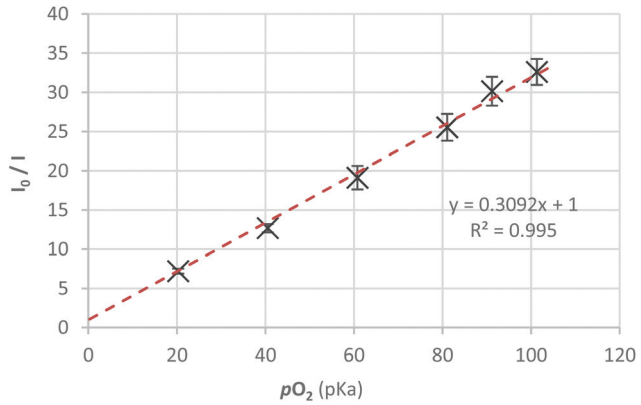

Fig. 9 Stern–Volmer plot of the O_2 sensitive phosphorescence peak at 645 nm against varying pO_2. K_{sv} = 0.309 kPa^{-1}. Overlap from the 515 nm peak was subtracted from intensity values before plotting.

The intensity change for the 645 nm peak for varying concentrations of O_2 is shown in Fig. 9, along with a theoretical Stern–Volmer plot. The overlap from the 515 nm peak shown in Fig. 6 and 7 was removed from 645 nm intensity measurements by subtracting an empirically found factor of 3.8×10^{-3} multiplied by the intensity measured at 515 nm. Figure errors and K_{sv} were found in the same way as for Fig. 8. Again, measurements correspond well to theoretical predictions, although the small differences in values for high O_2 concentrations are not always distinguishable over errors. The value of K_{sv} was found to be 0.309 kPa^{-1} in this case.

In order to investigate the O_2 cross-sensitivity to CO_2 measurements, the intensity change for the CO_2 sensitive 539 nm peak was measured as for Fig. 5, but with varying concentrations of O_2. The results are shown in Fig. 10. Intensity changes are very small in comparison to varying CO_2 concentrations and most of them do not show significant change outside of errors. It can be concluded that the CO_2 sensitive peak at 539 nm does not have significant cross-sensitivity to O_2.

Similarly, the CO_2 cross-sensitivity to O_2 measurements was investigated by measuring the intensity change of the O_2 sensitive peak at 645 nm whilst varying the concentration of CO_2.

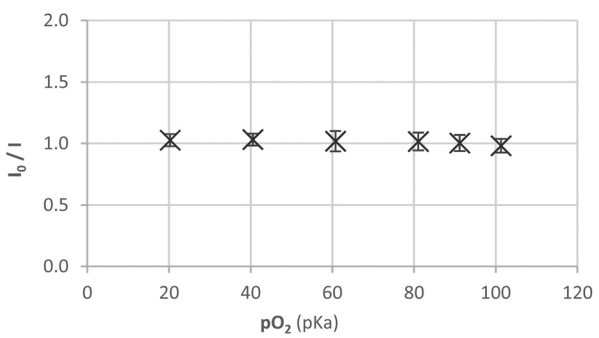

Fig. 10 Cross-sensitivity of the CO_2 sensitive peak at 515 nm to varying pO_2. I_0/I values were calculated in the same way as for Fig. 8.

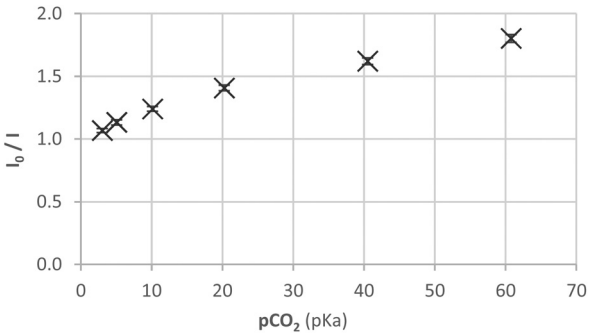

Fig. 11 Cross-sensitivity of the O_2 sensitive peak at 645 nm to varying pCO_2. I_0/I values were calculated in the same way as for Fig. 9.

The results are shown in Fig. 11. These results do show a cross-sensitivity to CO_2 which, while small in comparison to the sensitivity to O_2, is still significant. They also deviate from a linear Stern–Volmer plot.

5. Discussion and conclusion

The purpose of this study was to produce and test a phosphorescence chemical coating capable of responding separately to partial pressure of oxygen (pO_2) and partial pressure of carbon dioxide (pCO_2). A novel fibre-optic sensor was produced which included a chemical coating combining the pCO_2 sensitive molecule HPTS with the pO_2 sensitive molecule PtOEP.

The results show that the two fluorescent chemicals can be combined together without a problematic interaction. In early testing the $EMIMBF_4$ would sometimes form a solid precipitate when added to the mixture, requiring an adjustment of the concentrations. The process described allowed both fluorescent chemicals, the phase transfer and stabilising agents needed for optimal performance, and a coating polymer could all be combined within a single solution.

Further, the peaks of the two fluorescent chemicals can be clearly distinguished from one another and both remain able to fluoresce when mixed with the other. The addition of PtOEP did cause a dip in the HPTS phosphorescence peak at around 539 nm, shifting its intensity maximum from 520 nm to 515 nm. It is possible that this was caused by a non-fluorescent absorption from PtOEP molecules, but the peak could still clearly be distinguished with the new maximum.

The CO_2 sensitive phosphorescence peak was significantly wider than the O_2 sensitive peak at 645 nm, and overlapped it slightly. It was necessary to subtract this overlap from O_2 measurements. However, this did not result in a significant issue as the intensity of the overlap was proportional to the intensity of the 515 nm peak, which was measured through the testing. The 645 nm peak, being narrower and less intense, did not noticeably overlap with the centre of the 515 nm peak.

The two phosphorescence peaks were clearly shown to respond to their respective target, pO_2 and pCO_2, decreasing in intensity with increasing partial pressure as predicted by the

Stern–Volmer relationship. Both peaks showed good correspondence to predictions in isolation, allowing calibration constants of 0.0384 kPa^{-1} and 0.3092 kPa^{-1} for CO_2 and O_2 respectively.

While CO_2 measurements showed little or no cross-sensitivity to O_2, there was some cross-sensitivity the other way. The highest cross sensitivity was measured at 5.1 pK_a CO_2, which effected the 645 nm measurement equivalent to 0.43 pK_a of O_2, a ratio of 0.08 : 1. The lowest was measured at 61 pK_a which effected the 645 nm measurement equivalent to 23.5 pK_a of O_2, a ratio of 0.043 : 1. However, this cross-sensitivity appeared to follow a predictable pattern across pCO_2 values, allowing it to be subtracted from pO_2 measurements. pO_2 measurements must therefore be corrected for both overlap from the 515 nm peak and for cross-sensitivity to pCO_2. However, both are based on the 515 nm measurement which is independent of pO_2 and is measured throughout use.

The spectra observed for the CO_2 and the O_2 sensitive peaks of the combined mix are similar to those observed in isolation by previous studies, and similarly linear sensitivity plots were recorded.[1,4] However single sensors have typically shown significantly faster response times than those presented here. With an integration time of 50 ms and averaging over 100 measurements, the combined sensor had a response time of a little over 5 s, whereas Chu *et al.*[4] achieved pCO_2 measurements in 1.7 s and Chen *et al.*[15] achieved pO_2 response times below 50 ms. However it is important to note that these studies were aimed at optimising existing techniques of single measurements in isolation, whereas this study is the first to present combined measurements in this manner.

To conclude, this study demonstrates a new chemical compound that combines two fluorescent materials sensitive to pO_2 and pCO_2 respectively. The two materials fluoresce in different parts of the visible spectrum, allowing the signals to be distinguished and pO_2 and pCO_2 to be measured simultaneously. The pCO_2 sensitive peak slightly overlaps the pCO_2 sensitive peak and there is some cross-sensitivity from pCO_2 to pO_2.

Combining the two sensing materials presented many hurdles, depending on the concentrations and chemicals used, solid components would not dissolve, fluorescent intensity would decay too rapidly for practical use, or crystals would form preventing the mix to be used as a coating. However, after careful testing it proved to be possible to produce a mixture which in which both the pO_2 and the pCO_2 sensitive reactions could take place, and which could be successfully coated onto a surface such as an optical fibre.

The compound presents new opportunities for use in medical sensors. The key advantage of this sensor is its small size and relative simplicity compared to the two separate sensors that would otherwise be required. As the two fluorescent molecules are excited by the same wavelength, only a single light source is required. Coated onto the tip of an optical fibre, it can allow pCO_2 and pO_2 to be monitored simultaneously in remote locations such as the gastrointestinal tract. Alternatively a larger coating area could be used for a potentially increase sensitivity if accessing a remote location is not required.

The intensity of the fluorescent peaks may be measured using a spectrometer as in this study, or with optical filters and photodiodes. It may also be possible to improve the performance of the pO_2 measurements by using fluorescent lifetime measurements, which will be the focus of future investigations. This novel compound has great potential which we expect to be important to a wide range of future applications.

Acknowledgements

This report is independent research funded by the National Institute for Health Research (Invention for Innovation (i4i) program): *Development of a Multi-Parameter Oesophageal Sensor for the Early Detection of Multiple Organ Dysfunction Syndrome (MODS)*, Ref: II-LA-0313-20006. The views expressed in this publication are those of the author(s) and not necessarily those of the NHS, the National Institute for Health Research or the Department of Health.

References

1 J. Jiang, L. Gao, W. Zhong, S. Meng, B. Yong, Y. Song, X. Wang and C. Bai, Development of fiber optic fluorescence oxygen sensor in both in vitro and in vivo systems, *Respir. Physiol. Neurobiol.*, 2008, **161**, 160–166.

2 X. Yang, L. Peng, L. Yuan, P. Teng, F. Tian, L. Li and S. Luo, Oxygen gas optrode based on microstructured polymer optical fiber segment, *Opt. Commun.*, 2011, **284**, 3462–3466.

3 J. J. D. M. Hickey, J. P. Phillips and P. A. Kyriacou, Fiber-optic fluorescence-quenching oxygen partial pressure sensor using platinum octaethylporphyrin, *Appl. Opt.*, 2016, **55**(21), 5603–5609.

4 C.-S. Chu and Y.-L. Lo, Fiber-optic carbon dioxide sensor based on fluorinated xerogels doped with HPTS, *Sens. Actuators, B*, 2008, **129**(1), 120–125.

5 P. K. Contreras-Gutierrez, S. Medina-Rodríguez, A. L. Medina-Castillo, J. F. Fernandez-Sanchez and A. Fernandez-Gutierrez, A new highly sensitive and versatile optical sensing film for controlling CO2 in gaseous and aqueous media, *Sens. Actuators, B*, 2013, **184**, 281–287.

6 H. Segawa, E. Ohnishi, Y. Arai and K. Yoshida, Sensitivity of fiber-optic carbon dioxide sensors utilizing indicator dye, *Sens. Actuators, B*, 2003, **94**, 276–281.

7 T. Jarm, G. Sersa and D. Miklavcic, Oxygenation and blood flow in tumors treated with hydralazine: Evaluation with a novel luminescence-based fiber-optic sensor, *Technol. Health Care*, 2002, **10**, 363–380.

8 M. Urano, Y. Chen, J. Humm, J. A. Koutcher, P. Zanzonico and C. Ling, Measurements of Tumor Tissue Oxygen Tension Using a Time-Resolved Luminescence-Based Optical OxyLite Probe: Comparison with a Paired Survival Assay, *Radiat. Res.*, 2002, **158**, 167–173.

9 Oxford Optronix Ltd., *Oxford Optronix, Sensors, Sensors for Oxygen Monitors*, [Online]. Available: http://www.oxford-optronix.com/sensor12/sensor-for-Oxygen-Monitors.html. [Accessed 18th March 2016].

10 F. Formenti, R. Chen, H. McPeak, M. Matejovic, A. D. Farmery and C. E. Hahn, A fibre optic oxygen sensor that detects rapid PO2 changes under simulated conditions of cyclical atelectasis in vitro, *Respir. Physiol. Neurobiol.*, 2014, **191**, 1–8.

11 X. Zhang, W. Xuan, P. Yin, L. Wang, X. Wu and Q. Wu, Gastric tonometry guided therapy in critical care patients: a systematic review and meta-analysis, *Crit. Care*, 2015, **19**, 22.

12 V. B. Sivarajan and A. D. Bohn, Monitoring of standard hemodynamic parameters: Heart rate, systemic blood pressure, atrial pressure, pulse oximetry, and end-tidal CO_2, *Pediatr. Crit. Care Med.*, 2011, **14**(5), S51–S61.

13 S. Hendrik, F. S. Magnet, M. Dreher and W. Windisch, Transcutaneous monitoring as a replacement for arterial PCO 2 monitoring during nocturnal non-invasive ventilation, *Respir. Med.*, 2011, **105**(1), 143–150.

14 J. E. Cotes, C. J. David and M. R. Miller, *Lung function: physiology, measurement and application in medicine*, John Wiley & Sons, Hoboken, USA, 2009.

15 R. Chen, A. D. Farmery, A. Obeid and C. E. W. Hahn, A Cylindrical-Core Fiber-Optic Oxygen Sensor Based on Fluorescence Quenching of a Platinum Complex Immobilized in a Polymer Matrix, *IEEE Sens. J.*, 2012, **12**(1), 71–75.

16 X. Yang, L. Peng, L. Yuan, P. Teng, F. Tian, L. Li and S. Luo, Oxygen gas optrode based on microstructured polymer optical fiber segment, *Opt. Commun.*, 2011, **284**, 3462–3466.

17 R. M. Bukowski, R. Ciriminna, M. Pagliaro and F. V. Bright, High-Performance Quenchometric Oxygen Sensors Based on Fluorinated Xerogels Doped with [Ru(dpp)3]2+, *Anal. Chem.*, 2005, **77**, 2670–2672.

18 P. K. Contreras-Gutierrez, S. Medina-Rodríguez, A. L. Medina-Castillo, J. F. Fernandez-Sanchez and A. Fernandez-Gutierrez, A new highly sensitive and versatile optical sensing film for controlling CO_2 in gaseous and aqueous media, *Sens. Actuators, B*, 2013, **184**, 281–287.

19 H. Segawa, E. Ohnishi, Y. Arai and K. Yoshida, Sensitivity of fiber-optic carbon dioxide sensors utilizing indicator dye, *Sens. Actuators, B*, 2003, **94**, 276–281.

20 J. F. FernandezSanchez, R. Cannas, S. Spichiger, R. Steiger and U. E. Spichiger-Keller, Optical CO_2-sensing layers for clinical application based on pH-sensitive indicators incorporated into nanoscopic metal-oxide supports, *Sens. Actuators, B*, 2007, **128**, 145–153.

21 O. Oter, K. Ertekin and S. Derinkuyu, Ratiometric sensing of CO_2 in ionic liquid modified ethyl cellulose matrix, *Talanta*, 2008, **76**, 557–563.

22 L. J. Crawford and N. R. Edmonds, Calculation of thickness for dip coated antireflective films, *Thin Solid Films*, 2006, **515**, 907–910.

23 M. M. Chen, X. M. Zhang, J. P. Ma, S. C. Chen, W. X. Chen and L. F. Feng, Experimental study on film thickness and the problem of free surface film flow in dip coating, *Asia–Pac. J. Chem. Eng.*, 2016, **11**, 695–704.

24 A. Thakur, P. Thakur and K. Yadav, Thickness Dependent Optical Properties of PEMA and $(PEMA)_{0.85}/(ZnO)_{0.15}$ Nanocomposite Films Deposited by Spray Pyrolysis Technique on ITO Substrate, *AIP Conf. Proc.*, 2016, **1728**, 020412, DOI: 10.1063/1.4946463.